Available online at www.sciencedirect.com
SCIENCE DIRECT
Biochemical Pharmacology 70 (2005) 1458–1468
Biochemical Pharmacology
www.elsevier.com/locate/biochempharm

Determination of apoptosis, uracil incorporation, DNA strand breaks, and sister chromatid exchanges under conditions of thymidylate deprivation in a model of BER deficiency

Li Li, Ellen E. Connor, Sondra H. Berger, Michael D. Wyatt *

Department of Basic Pharmaceutical Sciences, College of Pharmacy, University of South Carolina, Columbia, SC 29208, USA

Received 22 July 2005; accepted 25 August 2005

Abstract

Thymidylate synthase (TS) is an important target of several chemotherapeutic agents. During TS inhibition, dTTP levels decrease with a subsequent increase in dUTP. Uracil incorporated into the genome is removed by base excision repair (BER). BER has been hypothesized to play a role in the response to thymidylate deprivation, despite a lack of direct evidence. We previously found that β-pol null murine fibroblasts were ∼six-fold more resistant than wild-type cells to raltitrexed, a folate-based inhibitor specific for TS. In this study, a number of endpoints were determined to understand the influence of BER and β-pol during raltitrexed treatment. Raltitrexed induced apoptosis in wild-type cells to a greater extent than in β-pol null cells. A PARP inhibitor decreased the sensitivity to raltitrexed, although the extent was not different between wild-type and β-pol null cells. No evidence was seen for extensive strand break formation that preceded apoptosis, although raltitrexed induced more sister chromatid exchanges in wild-type cells. Increased levels of uracil in DNA were detected following treatment in wild-type and β-pol null cells. However, uracil levels were only ∼two-fold higher in DNA from treated cells compared to untreated. Uracil DNA glycosylase activity was slightly higher in β-pol null cells, although not sufficiently different to explain the difference in sensitivity to raltitrexed. Taken together, the data suggest that the sensitivity of the wild-type cells to raltitrexed is not associated with activation of PARP-1 dependent BER, extensive uracil incorporation into DNA and persistent strand breaks, but rather with changes suggestive of DNA recombination.

Keywords: Raltitrexed; DNA repair; Thymineless stress; Cancer chemotherapy; Base excision repair; DNA polymerase β

1. Introduction

Thymidylate synthase (TS) is an important therapeutic target for several classes of antineoplastic drugs such as 5-fluorouracil (5-FU) and raltitrexed (Tomudex, RTX). RTX is a folate-based analogue that is specific for TS, whereas 5-FU has multiple mechanisms of action, including the inhibition of TS [1]. TS catalyzes the methylation of dUMP to TMP using N_5,N_{10}-methylenetetrahydrofolate as a coenzyme, which provides the only de novo source of TMP for DNA synthesis and repair. Although the precise mechanism of cytotoxicity has yet to be identified, nucleotide pool imbalance, cell cycle arrest, and DNA strand breaks have been reported [2]. TMP levels dramatically decrease with a subsequent increase in dUTP levels during TS inhibition, which presumably leads to uracil incorporation into DNA. Base excision repair (BER) purges uracil from the genome. However, under conditions of thymidylate deprivation, uracil reincorporation during repair synthesis would then lead to futile cycles of repair [2].

Interestingly, there is little direct evidence for futile cycling of BER during thymidylate deprivation induced by chemotherapeutics [2]. Studies in this regard have focused on two key enzymatic activities that combat the accumulation of uracil in DNA, dUTPase and uracil DNA glycosylase (below). The activity of dUTPase preempts uracil incorporation into DNA by hydrolyzing dUTP to dUMP. Studies that manipulated dUTPase levels during

Abbreviations: AP site, apurinic/apyrimidinic (abasic) site; 3-AB, 3-aminobenzamide; BER, base excision repair; 5-FU, 5-fluorouracil; FdUrd, 5-fluoro-2′-deoxyuridine; MEFs, murine embryonic fibroblasts; PARP, poly-ADP ribose polymerase; PFGE, pulsed-field gel electrophoresis; β-pol, DNA polymerase β; RTX, raltitrexed (Tomudex); SCE, sister chromatid exchange; TS, thymidylate synthase; UDG, uracil DNA glycosylase

* Corresponding author. Tel.: +1 803 777 0856; fax: +1 803 777 8356.
E-mail address: wyatt@cop.sc.edu (M.D. Wyatt).

0006-2952/$ – see front matter © 2005 Elsevier Inc. All rights reserved.
doi:10.1016/j.bcp.2005.08.016

chemotherapy-induced thymidylate deprivation indicate that dUTPase activity can delay death [3–7]. However, the time dependence implied that cytotoxicity did not ultimately depend on the DNA damage resulting from uracil incorporation [5,7]. For example, overexpression of dUTPase significantly reduced the cytotoxicity of a 24 h but not a 48 h exposure to ZD9331, a folate-based inhibitor of TS [7]. Furthermore, in some cell types, death was seen in TTP-depleted cells despite little or no dUTP accumulation [8], while other studies have implicated changes in dATP levels [9].

At least four distinct genetic loci in humans encode for uracil DNA glycosylases [10]. The *ung* genetic locus encodes mitochondrial (UNG1) and nuclear (UNG2) forms of uracil DNA glycosylase; the nuclear form of UDG appears to counteract uracil misincorporation during replication [10,11]. Studies examining the role of UDG have not clearly indicated that uracil excision significantly contributes to cell death induced by TS inhibitors. UDG overexpression did not affect either sensitivity to RTX following longer drug incubation times or clonogenicity, although UDG overexpressing clones were more sensitive following a 24 h treatment with RTX [12]. $Ung^{+/+}$ and $Ung^{-/-}$ MEFs showed no difference in the cytotoxic effects of 5-FU or fluorodeoxyuridine (FdUrd, the deoxynucleoside derivative of 5-FU) following 72 h exposure, despite an increased accumulation of AP sites and reduced proliferation in treated $Ung^{-/-}$ cells [13]. In *Saccharomyces cerevisiae*, inactivation of UDG resulted in resistance to shorter but not prolonged exposures to antifolate-based inhibitors [6]. Taken together, the above studies suggest that the effect of uracil misincorporation and its removal on survival is sensitive to the duration of treatment and recovery. A further complication has been the chemotherapeutic utilized, namely nucleotide-based or folate-based inhibitors of TS. The folate-based inhibitors of TS such as RTX appear to be specific for TS, while FdUrd can also be incorporated into DNA and 5-FU has additional RNA-directed effects [1]. Mismatch repair has been implicated in the recognition of 5-FU in DNA paired opposite guanine [14]. Furthermore, 5-FU paired opposite guanine in DNA appears to be a target for the TDG and MBD4 DNA glycosylases [15,16].

Our investigations seek to better define the role of BER during RTX-induced thymidylate deprivation. Due to the redundancy of mammalian uracil DNA glycosylase activities, we chose to look downstream in the BER pathway. DNA polymerase β (β-pol) performs two enzymatic funtions in mammalian short-patch BER, namely DNA synthesis to fill the gap, and dRP lyase to remove the dRP group [17,18]. We previously reported that wild-type MEFs are significantly more sensitive to RTX and FdUrd than β-pol null MEFs [19]. In contrast, the β-pol null MEFs are sensitive to alkylating agents, which produce damage that is repaired by BER [17,20,21]. The MEF model was chosen because we are examining a DNA repair pathway and human tumor cell lines are known for their inherent genomic instability. The aim of the current study was to investigate the mechanism of β-pol mediated sensitivity in the cellular response to TS inhibition by RTX.

2. Materials and methods

2.1. Drugs and cell culture

Raltitrexed (RTX) was generously supplied by AstraZeneca, U.K. Sulforhodamine B (SRB) and bromodeoxyuridine (BrdUrd) were purchased from Sigma (St. Louis, MO). Colcemid was purchased from Invitrogen (Carlsbad, CA). MB16tsa (wild-type) and MB19tsa (β-pol null) mouse embryonic fibroblasts (MEFs) were obtained from ATCC and were maintained in DMEM (Invitrogen) supplemented with 10% regular or dialyzed fetal bovine serum (Hyclone, Logan, UT) and 1% penicillin/streptomycin (Sigma) at 34 °C in a humidified 5% CO_2 incubator. We have verified that the wild-type and β-pol null cells are uninfected with mycoplasma. The 19HB3 cells were derived from the MB16tsa cells and express FLAG-tagged human DNA polymerase β [21,22]. The 19HB3 cells were a kind gift from Dr. Robert Sobol (University of Pittsburgh Cancer Institute). All cell lines were immortalized with SV40 T antigen [20,21].

2.2. Cytotoxicity of RTX in the presence of the PARP inhibitor 3-aminobenzamide (3-AB)

Cytotoxicity was performed by SRB colorimetric assay as described previously [19]. In brief, ~500 cells were plated on 96-well plates 24 h prior to treatment. The cells were treated with various concentrations of RTX for 24 h in the presence or absence of 3 mM 3-AB, then grown in media free of RTX but containing 3 mM 3-AB for 3 days. Cells were then fixed, washed, and stained. Absorbance was measured using a plate reader at 560 nm (Bio-Tek UV808 Microplate Reader, Winooski, VT).

2.3. Caspase-3 activity assay

Caspase-3 activity was measured in intact cells by a Caspase-Glo luminescence assay (Promega, Madison, WI). Cells were seeded into 96-well plates 24 h before treatment, and were then exposed to RTX at the concentrations and time points indicated in the text. Following 24 h treatment, the drug-containing media was replaced with drug-free media. At the time points listed, an equal volume of caspase-3 reagent was added to the cells. After 1 h incubation, luminescence was measured using a plate reader (Fluostar, BMG Technologies, Raleigh, NC). Relative Caspase-3 activity is expressed as fold induction compared to untreated control cells.

2.4. PARP cleavage

PARP cleavage was assessed by immunoblotting. Cells were exposed to 10 nM RTX for 24 h, and then incubated in drug-free media. At the times indicated, the cells were harvested by trypsinization. Cellular extracts were obtained by lysing the cells in ice-cold lysis buffer, followed by centrifugation at 10250 *g* for 10 min [19]. Protein content was determined by a BCA assay (Pierce, Rockford, IL). Total protein (30 μg) was separated by 10% SDS-PAGE, and transferred to Immobilon-P membranes (Millipore, Billerica, MA). After blocking, the membrane was incubated with antibodies against full-length and cleaved PARP or β-actin (Abcam, Cambridge, MA). PARP and β-actin (loading control) were visualized with horseradish peroxidase-conjugated anti-rabbit (for PARP) or anti-mouse (for β-actin) IgG secondary antibody and the ECL advance detection kit (Amersham Biosciences, Piscataway, NJ).

2.5. PFGE analysis

DNA double strand breaks were analyzed by pulsed field gel electrophoresis (PFGE). Cells were exposed to various doses of RTX for 24 h. Following drug removal, the cells were maintained in drug-free media. At the time indicated, the cells were harvested by trypsinization. The DNA plugs were prepared following the manufacturer's protocol (Bio-Rad, Hercules, CA). Each plug contained approximately 5×10^5 cells. DNA plugs were embedded into 1% agarose gels, and electrophoresed in 0.5 × TBE buffer for 24 h at 14 °C using a CHEF DR-II apparatus (Bio-Rad, Hercules, CA). The gel was run at 4 V/cm, with an initial switch time of 60 s and a final switch time of 240 s. The DNA was stained with syber green I dye (Molecular Probes, Eugene, OR), and visualized with a Bio-Rad Molecular Imager® FX and Quantity One® software.

2.6. Comet assay analysis

Following treatment and harvesting, cells were analyzed by comet assay as described [23]. Briefly, cell suspensions (2.5×10^4 cells/ml) were mixed with 1% low gelling type VII agarose at 40 °C, then pipetted onto precoated slides (Trevigen, Gaithersberg, MD). Once the agarose set, the slides were submerged in ice-cold lysis buffer (1% Triton X-100, 100 mM Na_2EDTA, 2.5 M NaCl, 10 mM Tris, pH 10.5). After lysis, slides were washed and submerged in alkali buffer (50 mM NaOH, 1 mM Na_2EDTA, pH 12.5) for 45 min. Electrophoresis was for 25 min at 0.6 V/cm. Slides were washed with a neutralization buffer (0.5 M Tris–HCl, pH 7.5), followed by a PBS wash, then dried overnight. The slides were rehydrated with distilled water, stained with propidium iodide (2.5 μg/ml) for 30 min, then destained for 30 min in water. Comets were visualized with a Nikon E600 microscope with a 565 nm dichromic mirror, 510–560 nm excitation filter and 590 nm barrier filter. Comets were analyzed with as described [24].

2.7. Uracil misincorporation

Uracil levels in DNA were analyzed as described [25]. Briefly, 24 h after seeding, the cells were exposed to 10 nM RTX for 24 h, then washed of drug-containing media. At the times listed, the cells were harvested by trypsinization. Genomic DNA was extracted from the cell pellets using a DNAeasy kit (Qiagen, Valencia, CA), and quantitated by a Picogreen dye assay (Molecular Probes, Eugene, OR). To release genomic uracil from DNA, 3 μg DNA was incubated with 0.2 Units of UDG (NEB, Beverley, MA) for 1 h at 37 °C. Following digestion, 50 pg of a labeled uracil internal standard ($^{13}C_4H_4O_2{}^{15}N_2$; Cambridge Isotope Laboratories, Andover, MA) was added to each tube. The samples were then vacuum dried, and derivatized with 3,5-bis(trifluoromethyl)benzyl bromide for 25 min at 30 °C. The samples were analyzed by GC–MS in negative chemical ionization mode on a 5973N GC–MS (Agilent, Palo Alto, CA). The samples were separated on a HP-5MS capillary column (30 m × 0.25 mm × 0.25 μm; Agilent). The oven temperature was initiated at 100 °C, holding for 1 min, ramping to 240 °C at 25 °C/min, and then ramping to 280 °C at 20 °C/min. The GC–MS interface temperature was set to 280 °C. The mass spec conditions were as follows: NCI mode; SIM at *m/z* 337 and 343; ion source temperature, 140 °C; quadrapole temperature, 100 °C; and methane was used as reagent gas.

2.8. UDG activity

Uracil excision activity for the wild-type and β-pol null cell extracts was measured using an oligodeoxynucleotide-based assay. An oligo containing a single uracil (5′-CGG ATC CTC AUG TGA ATT CC (IDT, Coralville, IA)) was 5′-end labeled with ^{32}P and annealed to its complement to produce a duplex oligo with a U:A base pair. The uracil excision assay was carried out by incubation of the duplex oligo with 2 μg of cell extracts in buffer (20 mM Tris, 100 mM KCl, 5 mM EDTA, 1 mM EGTA, 5 mM 2-mercaptoethanol, pH 7.2) at 37 °C for the times listed. The reaction products were separated on a denaturing 20% polyacrylamide gel. The gels were visualized and quantified with a Bio-Rad Molecular Imager® FX and Quantity One® software.

2.9. Sister chromatid exchange

Cells were treated for 24 h with 4 nM RTX. Following drug removal, cells were further incubated in media containing 10 μM BrdUrd for 24 h. Colcemid (0.1 μg/ml) was added 2 h prior to the end of the 24 h recovery. The cells were harvested by mitotic shakeoff, resuspended, and fixed in Carnoy's solution. To produce "harlequin"

chromosomes, a modified fluorescence plus Giemsa technique was used [26]. At least 1000 chromosomes were counted per slide and SCE events were calculated as SCEs per chromosome.

3. Results

3.1. Cytotoxicity of RTX

We previously reported that β-pol null cells were six-fold resistant to RTX compared to wild-type cells following a 24 or 48 h exposure [19]. The phenotype was also seen in cells grown in dialyzed serum, which suggested that the difference in sensitivity was not due to a difference in the ability to salvage thymidine from regular serum. To determine whether the phenotype might be affected by the duration of exposure, the wild-type and β-pol null cells were exposed to RTX for 96 h in media containing dialyzed serum. Fig. 1A shows that the wild-type cells remained sensitive relative to the β-pol null cells (IC_{50} of 2 nM versus 12 nM, respectively). In our previous report, we found that wild-type cells expressing siRNA against β-pol were resistant to RTX, relative to wild-type controls [19]. In order to further confirm the β-pol dependence of the observed phenotype, we examined the toxicity of RTX in the 19HB3 cell line. The 19HB3 cells, which were derived from the β-pol null cells, express Flag-tagged human DNA polymerase β [21,22]. Fig. 1B shows that the 19HB3 cells were more sensitive than the β-pol null cells to a 24 h exposure to RTX (IC_{50} of 11 nM versus 27 nM, respectively), although they do not fully regain the sensitivity of the wild-type cells (5.5 nM) [19]. Previous reports have noted that prunasin can act as an inhibitor of β-pol [27,28]. We examined the influence of prunasin on the sensitivity of the wild-type and β-pol null cells to RTX. However, the presence of prunasin did not alter the sensitivity of either cell line to RTX (data not shown).

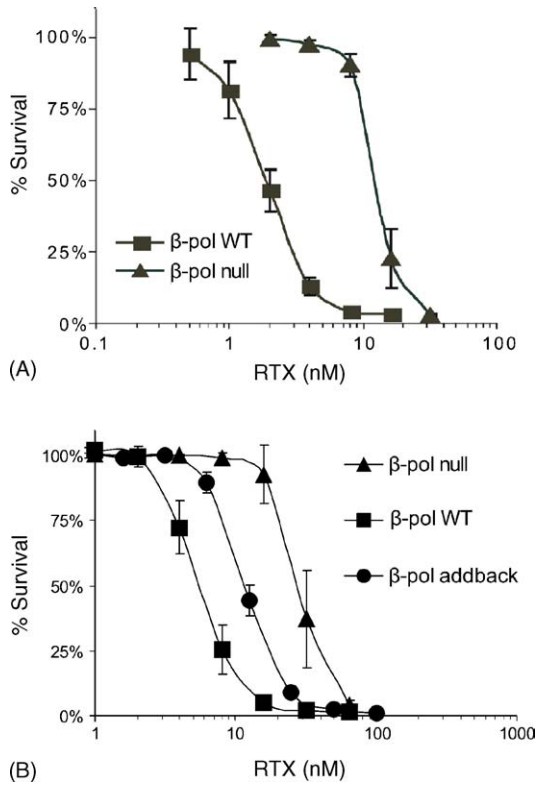

Fig. 1. Cytotoxicity in wild-type and β-pol null MEFs treated with RTX. (A) Wild-type (■) and β-pol null (▲) cell lines were exposed to RTX in media containing dialyzed serum 24 h post-plating in 96-well plates. After 96 h exposure, cytotoxicity was determined by SRB assay (Section 2). (B) Wild-type cells (■), β-pol null cells (▲), and β-pol null cells expressing human β-pol (●) were exposed to RTX for 24 h in media containing dialyzed serum 24 h post-plating in 96-well plates. After exposure, drug-containing media was removed. Cytotoxicity was determined following 3 days recovery by SRB assay (Section 2). Results are shown as the percentage compared to untreated control and represent the average ± S.D. S.D. of three independent experiments.

3.2. Dose- and time-dependent induction of apoptosis by RTX

As part of investigating the potential mechanism of β-pol mediated sensitivity, we determined apoptosis induced by RTX in wild-type and β-pol null MEFs. Apoptosis was assessed by two commonly used markers, caspase-3 activation and cleavage of PARP. Caspase-3 activity was determined in intact cells by a sensitive luminescence assay. The dose-dependent caspase activation was determined in wild-type and β-pol null MEFs exposed to RTX for 24 h followed by 24 h incubation in drug-free media. As shown in Fig. 2A, caspase-3 activity was induced in a dose-dependent manner, and increased up to five-fold in the wild-type cells compared to untreated cells. Caspase-3 activity was not significantly activated in β-pol null cells following 5 or 10 nM RTX, whereas the highest dose of RTX shown (15 nM) induced caspase activity ∼two-fold. Treatment of β-pol null cells with an IC_{90} (50 nM) dose of RTX induced caspase activity >10-fold, which indicates that the difference in RTX sensitivity is not due to β-pol directly signaling to apoptosis (data not shown). We also measured the time-course of caspase-3 activation following 10 nM RTX treatment in the wild-type and β-pol null cells. A dose of 10 nM is the IC_{90} dose for wild-type cells. Fig. 2B shows caspase-3 activity in wild-type cells was ∼two-fold higher immediately following 24 h exposure to RTX, and continued to increase up to ∼five-fold induction by 24 h recovery. However, no significant induction of caspase-3 activity was observed at the same time points in β-pol null cells. To further confirm the induction of apoptosis, we detected the appearance of the cleaved form of PARP by western blot analysis. PARP-1, which has a role in BER (see next section), is cleaved by caspase-3 into an 85 kDa fragment during apoptosis. Consistent with caspase-3 activation, the

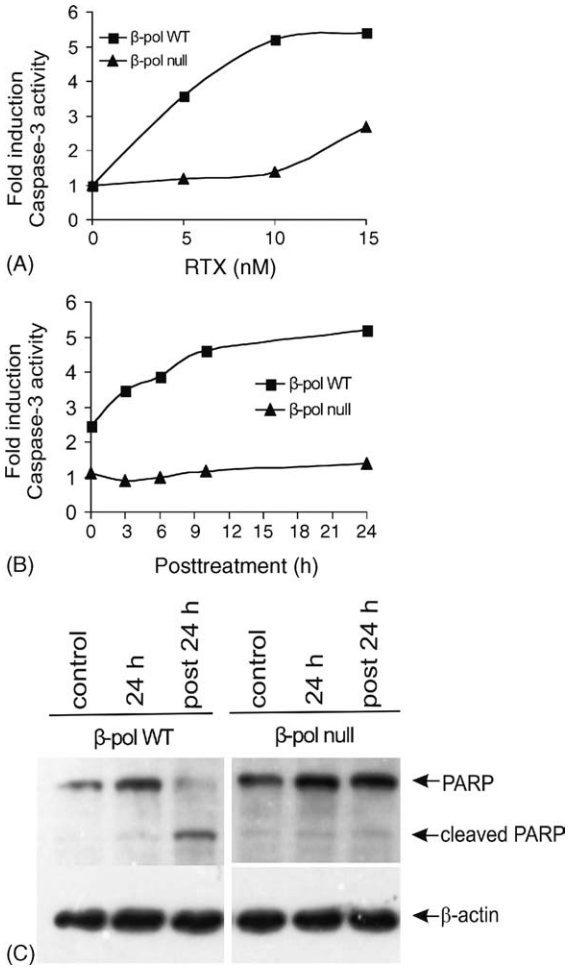

Fig. 2. Apoptosis induction by RTX in wild-type and β-pol null MEFs. Caspase-3 activity was measured in intact cells by a Caspase-Glo luminescence assay (A and B). Relative Caspase-3 activity is represented as fold induction compared to untreated control cells. The wild-type (■) and β-pol null (▲) cell lines were plated in 96-well plates 24 h prior to treatment in media containing dialyzed serum. (A) For the dose–response experiments, cells were exposed to doses of RTX for 24 h, followed by 24 h recovery in drug-free media. (B) For time-course experiments, cells were treated for 24 h with 10 nM RTX, and then incubated in drug-free media for 0, 3, 6, 10 or 24 h. (C) PARP cleavage induced by RTX was measured by immunoblotting. Wild-type and β-pol null cell lines were treated for 24 h with 10 nM RTX, and harvested immediately after 24 h treatment (24 h) or after 24 h recovery (post 24 h) in drug-free media. β-Actin was used as a loading control.

85 kDa fragment of PARP was observed following 24 h recovery in wild-type cells, whereas no PARP cleavage was observed in β-pol null cells (Fig. 2C). Cleaved PARP was not seen immediately after 24 h treatment of RTX in wild-type cells, presumably because caspase-3 activation is upstream of PARP cleavage. Lastly, there was no significant induction of full-length PARP protein levels during RTX treatment (Fig. 2C). Taken together, the data suggest that RTX treatment induced apoptosis in a time- and dose-dependent manner to a much greater extent in the wild-type cells, which was consistent with the cytotoxicity data [19].

3.3. The effect of a PARP inhibitor on cytotoxicity induced by RTX

There were several reasons to further investigate the potential influence of PARP-1 during RTX treatment in the wild-type and β-pol null cells. PARP-1 has been shown to be actively involved in BER and single strand break repair via its interactions with β-pol, DNA Ligase IIIα, and XRCC1 [29]. PARP-1 avidly binds to single-strand breaks, thus seeming to serve as a sensor of single strand breaks. Inhibitors of PARP render cells more sensitive to alkylating agents such as methylmethane sulfonate (MMS), although the precise mechanism by which this occurs is not clear [30,31]. Recent evidence also indicates that completion of BER in β-pol null cells is dramatically impaired in the absence of PARP-1 [32]. Lastly, PARP-1 is thought to play a role in cell death decisions, possibly via its ability to consume NAD^+ [33,34]. Therefore, the influence of the PARP inhibitor 3-aminobenzamide (3-AB) on the cytotoxicity induced by RTX was determined. The cells grown in media containing regular serum were exposed to RTX or MMS, and 3-AB was included during treatment and recovery at a constant concentration (3 mM). The dose of 3 mM for 3-AB was chosen based on previously published reports and by itself did not cause toxicity at this dose (data not shown). The inclusion of 3-AB significantly sensitized wild-type and β-pol null cells to the toxic effects of MMS (Fig. 3A). However, as shown in Fig. 3B, 3-AB decreased slightly the sensitivity of the MEFs to RTX. Furthermore, there was no difference between the wild-type and β-pol null cells in the extent of resistance to RTX induced by 3-AB. The effect of 3-AB on caspase-3 induction by RTX was measured in wild-type cells grown in media containing dialyzed serum. In agreement with the cytotoxicity results, the presence of 3 mM 3-AB diminished RTX-induced caspase-3 activity by 1.6-fold in the wild-type cells (data not shown). The results do not suggest that the relative sensitivity of wild-type cells to RTX is due to a PARP-dependent interaction with β-pol. The results also suggest against the possibility that RTX is directly inducing strand breaks that are recognized by PARP-1. However, PARP-1 may be playing a role in the decision to undergo cell death following RTX treatment in these cell lines.

3.4. DNA strand breaks following treatment with RTX

It has been suggested that cell death resulting from TS inhibition was due to an accumulation of DNA strand breaks [35–37]. However, DNA fragmentation has not uniformly correlated with death in response to folate-based TS inhibitors in all studies [5,38]. We felt it necessary to discriminate between strand breaks that might result from activation of DNA repair, and strand breaks associated with execution of cell death. To examine double strand breaks, we utilized pulsed field gel electrophoresis (PFGE), as was

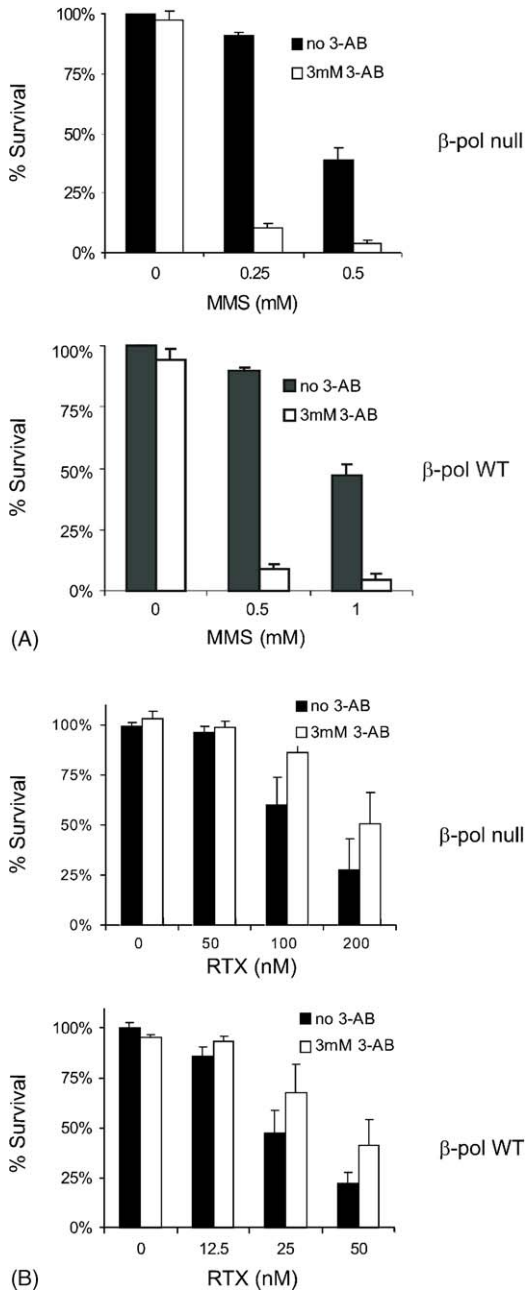

Fig. 3. Inhibition of PARP by 3-AB reduced the RTX-induced cytotoxicity in wild-type and β-pol null MEFs. Wild-type and β-pol null cell lines were exposed to drug at the doses shown in the absence (filled bar) or presence of 3-AB (3 mM, open bar) 24 h post-plating in 96-well plates in media containing regular serum. After exposure, drug-containing media was removed. Cytotoxicity was determined following 3 days recovery in either drug-free or 3-AB (3 mM) containing media. Data represent the average ± S.D. of three independent experiments. (A) Wild-type and β-pol null cell lines were exposed to MMS for 1 h at the doses shown in the absence (filled bar) or presence of 3-AB (3 mM, open bar). (B) Wild-type and β-pol null cell lines were exposed to RTX for 24 h at the doses shown in the absence (filled bar) or presence of 3-AB (3 mM, open bar).

used in a previous report [35]. The MEFs were exposed to various doses of RTX for 24 h, and then incubated in drug-free media for 24 h. As shown in Fig. 4, at concentration of 8 nM RTX, DSBs were detected in wild-type cells, but not in β-pol null cells. DSBs formation in β-pol null cells was

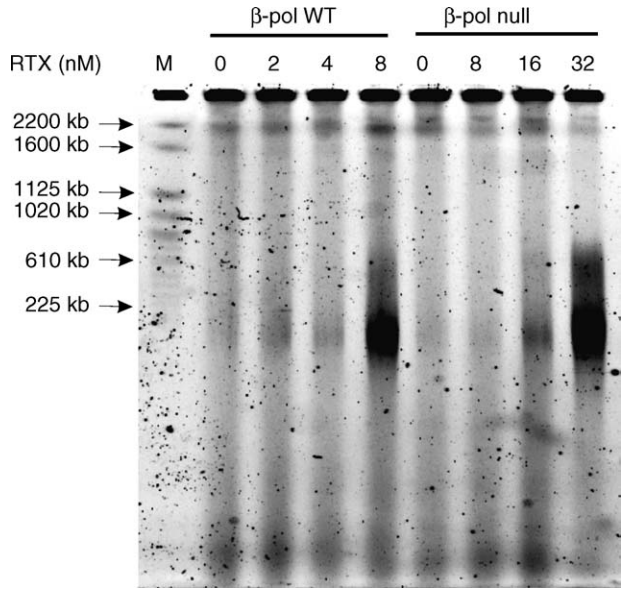

Fig. 4. DNA double strand breaks (DSBs) formation in wild-type and β-pol null cell lines treated with RTX. DNA double strand break formation was analyzed by pulsed field gel electrophoresis. Wild-type and β-pol null cell lines were exposed to the listed doses of RTX for 24 h, and harvested following 24 h recovery in drug-free media containing dialyzed serum. The figure shown is a representative experiment of three independent experiments. M: *S. cerevisiae* chromosomal marker (Bio-Rad).

only seen at a much higher concentration of RTX (32 nM). In both cell types, DSBs were only seen at RTX doses that were more toxic (>IC_{50}), which agreed with previous studies in three different colon cancer cell lines [35]. In order to detect an early onset of single strand breaks, the alkaline COMET assay was used. Interestingly, we did not detect significant single DNA strand breaks induced by RTX (data not shown). Specifically, cells were examined immediately following 12 or 24 h treatment. Cells were also examined at recovery time points of 6 or 24 h following 24 h treatment. In light of the time frame of caspase-3 activation seen above, the DSBs seen by PFGE analysis appear to be a result of apoptosis and not directly induced by RTX in this cell model.

3.5. Uracil in the genomic DNA of β-pol wild-type and null cells after RTX treatment

Uracil incorporation into DNA due to elevated dUTP levels has long been postulated as an important early event during chemotherapy-induced thymidylate deprivation [39]. We directly determined genomic uracil levels, by GC–MS, in wild-type and β-pol null cells before and after treatment with RTX [25]. As shown in Fig. 5, wild-type and β-pol null cells had a similar baseline level of 1.0 pg uracil/μg DNA prior to treatment. This level of genomic uracil was higher than that reported for human mononuclear blood cells grown in a high folate concentration (3 μM folate, 0.33 pg uracil/μg DNA), but less than in cells grown in folate deficient conditions (12 nM folate, 6.35 pg uracil/

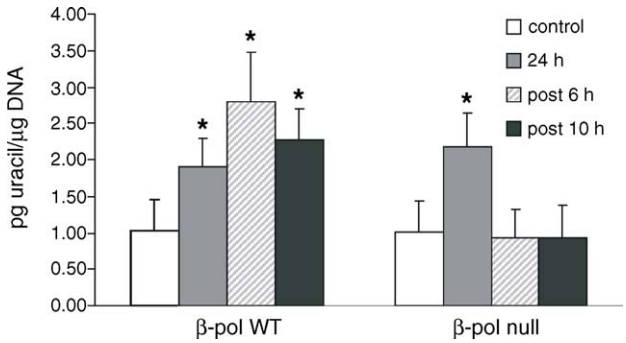

Fig. 5. Uracil levels in wild-type and β-pol null MEFs treated with RTX by GC–MS. Wild-type and β-pol null MEFs were exposed to 10 nM RTX for 24 h, and then incubated in drug-free media for 0, 6 or 10 h in dialyzed serum. Uracil levels in DNA were analyzed by GC–MS in negative chemical ionization mode (Section 2). The results were shown as the mean ± S.E. of three separate experiments. Control, untreated cells; 24 h time point, cells were harvested immediately after 24 h exposure to RTX; post, cells were incubated in drug-free media for 6 or 10 h after 24 h treatment with RTX. Each asterisk represents a significant difference compared to untreated control as measured by a student's *t*-test with *p*-values of <0.05.

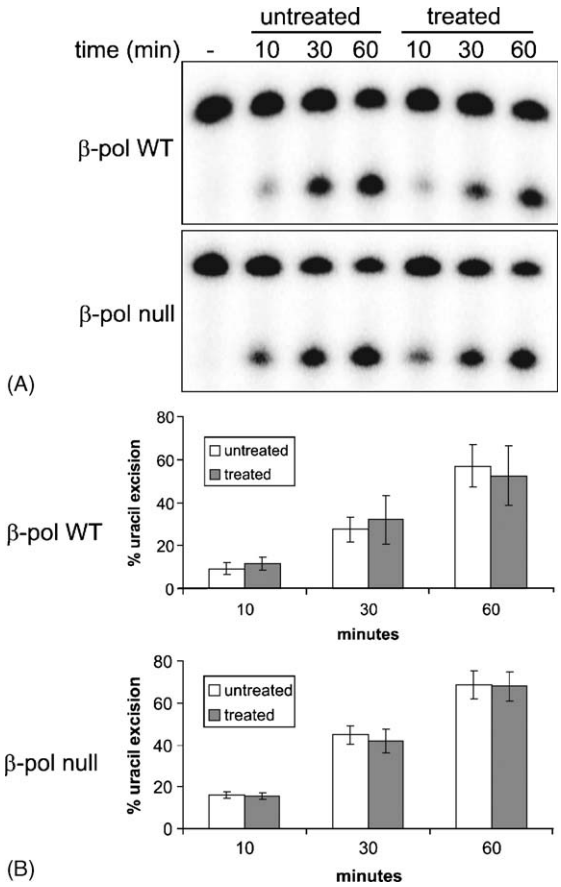

Fig. 6. UDG activity in wild-type and β-pol null MEFs before and after RTX treatment. UDG activity in wild-type and β-pol null cells was determined using an oligodeoxynucleotide-based assay (Section 2). Whole cell extracts were prepared from cells that were untreated or treated with 10 nM RTX for 24 h in media containing dialyzed serum. The uracil-containing oligo was incubated with extracts from wild-type and β-pol null cells for the times indicated. (A) A representative gel. Oligo not incubated with extracts is marked with dash. (B) The graphs show the averaged data from two to four experiments for each time point with standard deviations.

μg DNA) [25]. Following 24 h treatment with RTX, genomic uracil levels increased in both wild-type and β-pol null cells, but only by ∼two-fold (1.9 and 2.2 pg uracil/μg DNA, respectively). After 6 h recovery, the genomic uracil levels in wild-type cells rose to 2.8 pg uracil/μg DNA before dropping to 2.3 pg uracil/μg DNA. In contrast, genomic uracil levels returned to baseline levels in β-pol null cells during the recovery time points. It is interesting to note that uracil levels in DNA only reached a maximum of 2.8 pg uracil/μg DNA in the wild-type cells, despite a 24 h exposure to a toxic RTX dose, an amount that is less than the genomic uracil levels reported for human cells grown in folate deficient conditions (6.35 pg uracil/μg DNA) [25]. The data do not suggest that uracil incorporation into DNA is dramatically increased following exposure to toxic concentrations of RTX.

3.6. UDG activity in β-pol wild-type and null cells following RTX treatment

To determine whether the higher genomic uracil levels seen in wild-type cells might be due to an altered ability to remove uracil from DNA in the MEF cell lines, we examined UDG activity in the wild-type and β-pol null cells. Uracil DNA glycosylase activity was also examined after exposure to RTX, to determine whether RTX treatment might influence uracil DNA glycosylase activity. Uracil DNA glycosylase activity was determined by an oligodeoxynucleotide-based assay with cell extracts from cells before and after treatment with 10 nM RTX (Fig. 6). Interestingly, uracil DNA glycosylase activity appeared to be approximately two-fold higher in the β-pol null cells before and after treatment. However, there was no appreciable induction of uracil DNA glycosylase activity after RTX treatment in either wild-type or β-pol null cells. The reason for the difference in uracil DNA glycosylase activity is currently not known. The ∼two-fold drop in uracil levels seen in the β-pol null cells during recovery from RTX treatment might be explained by the ∼two-fold increase in uracil DNA glycosylase activity. However, the oligonucleotide-based assay only provides a measure of overall uracil DNA glycosylase activity, and does not distinguish between the different uracil DNA glycosylases (e.g., UDG, SMUG), nor between the nuclear and mitochondrial forms of UDG.

3.7. Sister chromatid exchange events induced by RTX in β-pol wild-type and null cells

Thymidylate deprivation induced by FdUrd has been reported to induce genetic recombination [40,41]. Although substantial strand break formation was not detected at earlier time points or lower doses of RTX (above), we sought to determine whether RTX might

Table 1
Sister chromatid exchanges per chromosome

	Untreated	4 nM RTX
Wild-type	0.127 ± 0.027[a]	0.188 ± 0.018[b]
β-Pol null	0.134 ± 0.022	0.148 ± 0.020

[a] SCE events/chromosome ± S.D. for three experiments.
[b] *p*-Value of 0.0061 as determined by student's *t*-test.

transiently induce strand break events that went undetected by Comet assay or PFGE. Sister chromatid exchanges (SCEs) are reciprocal exchanges of DNA between sister chromatids during S-phase [26]. The induction of SCEs by RTX was determined in the wild-type and β-pol null cells as a marker of strand breakage and repair events. Briefly, the cells grown in media containing dialyzed serum were treated with 4 nM RTX for 24 h, then allowed to recover for 24 h in RTX-free media containing bromodeoxyuridine (Section 2). It is necessary to use subtoxic doses of any drug to be evaluated by the SCE assay, so that the cells can complete the round of replication that produces differentially labeled sister chromatids. Table 1 shows that SCE events were induced by RTX in the wild-type cells at a dose of 4 nM. The results show that RTX can induce events that are presumed to be evidence of homologous recombination. The results also suggest that the presence of β-pol increases the occurrence of the events.

4. Discussion

The present studies were undertaken to investigate the basis for the relative resistance of mammalian cells deficient in β-pol [19]. In the present investigation, the wild-type cells were significantly more sensitive to apoptosis induction, which agreed with the cytotoxicity data. The time course data indicated that caspase-3 activation begins following 24 h exposure to toxic doses of RTX. The PARP inhibitor 3-AB was used to distinguish between the possible direct and indirect roles that PARP may play in the response to RTX treatment. PARP is known to be activated by single strand breaks and other aberrant DNA structures. The presence of 3-AB substantially increased the sensitivity of cells to MMS, regardless of β-pol status. MMS is known to produce alkyl base adducts that are repaired by BER. Therefore, a PARP inhibitor might be expected to heighten sensitivity to TS inhibitors, if extensive uracil incorporation and strand breaks result from TS inhibition. However, the presence of 3-AB increased resistance to RTX, which implies that PARP is negatively influencing survival following TS inhibition. Because 3-AB increased resistance equally in the wild-type and β-pol null cells, the sensitivity of the wild-type cells does not appear to depend on a β-pol dependent interaction with PARP. The protective effect of PARP inhibition following RTX treatment appears to be due to a delay or inhibition of death.

The specific role of uracil incorporation into DNA and uracil excision by BER during TS inhibition is not well understood. We directly determined uracil incorporation into DNA during RTX treatment and at early recovery times in the wild-type and β-pol null cells. Uracil incorporation was increased following RTX treatment in both cell types, but the levels of uracil incorporation only increased two to three-fold above a background of approximately 1 uracil per μg of genomic DNA. There was a difference in genomic uracil levels between wild-type and β-pol null cells during recovery, namely uracil levels in the null cells returned to levels seen in untreated cells, whereas the uracil levels in the wild-type cells remained elevated during recovery. The cause of the difference in uracil levels during recovery is not known but might be explained by the two-fold difference in UDG activity, or by the polymerase activity of β-pol in the wild-type cells that allows for incorporation of uracil during repair synthesis. Regardless, the differences in genomic uracil levels and uracil DNA glycosylase activity are not enough to account for the six-fold difference in sensitivity to RTX seen in the wild-type cells. Our results agree with other studies that suggest that uracil excision is not required to induce cell death during thymidylate deprivation [12,13,42]. TS deficient murine cells deprived of thymidine showed very little uracil incorporation into DNA [42]. UDG overexpression did not affect sensitivity to prolonged RTX exposures, although UDG overexpressing clones were more sensitive following a 24 h treatment with RTX [12]. There was no apparent difference in cytotoxicity between the $ung^{+/+}$ and $ung^{-/-}$ cells following a 72 h exposure to FdUrd, despite an *increase* in genomic uracil and AP sites and a delay in proliferation in the $ung^{-/-}$ cells [13]. The authors suggest that, in the absence of UDG, BER is less coordinated and efficient. Interpreting the impact of UDG-initiated BER on cell death induced by FdUrd is complicated by prolonged exposures and the recognition of 5-FU in DNA by mismatch repair and the TDG and MBD4 DNA glycosylases [14–16].

Initiating BER via DNA glycosylase activity in the absence of β-pol leads to numerous negative consequences [17,18,43]. Specifically, knocking out the DNA glycosylase MPG renders the β-pol null cells more resistant to the alkylating agent MMS [17]. Because the β-pol null cells are resistant to RTX and FdUrd, this suggests that extensive uracil excision to initiate BER is not occurring during thymidylate deprivation induced by these TS inhibitors (and/or that uracil incorporation is minimized by dUTPase). The data argue against a model of futile cycling whereby the toxicity stems from uracil excision that leads to the production of BER intermediates. It is not clear how loss of β-pol confers resistance to TS inhibitors in this model. β-Pol lacks a 3′–5′ proofreading exonuclease activity, and is significantly more error-prone than replicative polymerases [44]. The lower fidelity of β-pol might con tribute to genomic instability under conditions of

thymidylate deprivation and nucleotide imbalance. Furthermore, the sensitivity of the β-pol wild-type cells might derive from other interactions that determine the choice between short-patch and long-patch BER. For uracil that is misincorporated during replication, Long-patch BER appears to be preferred [11]. The presence of β-pol might, therefore, interfere with other repair machinery during the response to TLS.

The precise cause of the strand breaks following treatment with TS inhibitors in mammalian cells has been difficult to ascertain. Canman et al. examined FdUrd and a folate-based inhibitor of TS in three different colon cancer cell lines [3]. Using PFGE, they noted fragmentation corresponding to 50–200 kb, or 200 kb–5 Mb, depending on the cell line. They also noted that the fragmentation might be an apoptotic feature because it was not seen until drug doses that induced >80% cell death. Our results agree in that we saw fragmentation corresponding to 50–200 kb, but only at RTX doses that were very toxic to the wild-type and β-pol null cells. Other studies have measured strand breaks by comet assay or conventional gel electrophoresis, but the distinction was not made as to whether the strand breaks seen resulted from the induction of apoptosis [38,45,46]. Alternatively, the strand breaks observed following TS inhibition may be more apparent in human tumor cell lines, most of which are characteristically known to have an inherent chromosomal instability.

In our studies in diploid murine embryonic fibroblasts, strand break induction by RTX in the MEFs was not noted prior to the onset of apoptosis, as measured by comet assay, PFGE, and caspase-3 activity, respectively. However, sister chromatid exchanges were induced by subtoxic doses of RTX, which implies that a strand break event preceded the exchange and that recombinational repair mechanisms might be involved. Previous studies with high doses of RTX have shown that S-phase arrest occurs prior to the induction of p53 or DNA strand breaks, suggesting that thymidylate deprivation, not strand breaks, causes the initial arrest [38]. The source of the strand break leading to the SCE event at lower doses of RTX is not known, but extensive and persistent strand breaks were not detected at higher RTX doses where an S-phase arrest was seen in the MEFs ([19], and unpublished). The results suggest that the strand breaks associated with recombination events induced by lower doses of RTX are manifested by the progression from S-phase into G2/M. In contrast, higher drug doses induce a substantial S-phase arrest, which might induce a different cellular response that does not manifest in the appearance of extensive strand break formation until the induction of apoptosis.

Previous studies in *Escherichia coli* and *S. cerevisiae* provided reasonable evidence that uracil misincorporation and removal results in DNA strand breaks [47–51]. Interestingly, *resistance* to thymidylate deprivation has previously been noted in *S. cerevisiae* strains deficient in post-replicative repair [50]. Thymidylate deprivation induced by FdUrd in TS-deficient mouse cells that express a heterologous human TS resulted in the emergence of TS-deficient clones at a 10-fold higher frequency than that occurring spontaneously [41]. Using the heterologous human TS gene as a marker, specific deletions were observed that were consistent with the occurrence of homologous recombination at *Alu* sequences present within the TS gene. The data suggest that recombination can occur as a result of chemotherapy-induced thymidylate deprivation. The observations also suggest that DNA repair by recombination may play an important role in the response to TS inhibitors. We are in the process of investigating the influence of DNA recombination in response to chemotherapy-induced thymidylate deprivation.

Acknowledgements

This work was supported by NIH Grant Number R01 CA100450 from NCI and P20 RR-017698 from the COBRE Program of the National Center for Research Resources. AstraZeneca is acknowledged for the generous gift of raltitrexed. Dr. Robert Sobol is thanked for the generous gift of 19HB3 cells and helpful discussions. Dr. Alan Waldman is thanked for helpful discussions. Dr. Joseph Kosh is thanked for assistance with the GC–MS experiments.

References

[1] Longley DB, Harkin DP, Johnston PG. 5-Fluorouracil: mechanisms of action and clinical strategies. Nat Rev Cancer 2003;3(5):330–8.
[2] Aherne GW, Brown S. The role of uracil misincroporation in thymineless death. In: Jackman AL, editor. Anticancer Drug Development Guide: Antifolate Drugs in Cancer Therapy. Totowa, NJ: Humana Press Inc.; 1999. p. 409–21.
[3] Canman CE, Radany EH, Parsels LA, Davis MA, Lawrence TS, Maybaum J. Induction of resistance to fluorodeoxyuridine cytotoxicity and DNA damage in human tumor cells by expression of *Escherichia coli* deoxyuridinetriphosphatase. Cancer Res 1994;54(9):2296–8.
[4] Koehler SE, Ladner RD. Small interfering RNA-mediated suppression of dUTPase sensitizes cancer cell lines to thymidylate synthase inhibition. Mol Pharmacol 2004;66(3):620–6.
[5] Parsels LA, Parsels JD, Wagner LM, Loney TL, Radany EH, Maybaum J. Mechanism and pharmacological specificity of dUTPase-mediated protection from DNA damage and cytotoxicity in human tumor cells. Cancer Chemother Pharmacol 1998;42(5):357–62.
[6] Tinkelenberg BA, Hansbury MJ, Ladner RD. dUTPase and uracil-DNA glycosylase are central modulators of antifolate toxicity in *Saccharomyces cerevisiae*. Cancer Res 2002;62(17):4909–15.
[7] Webley SD, Welsh SJ, Jackman AL, Aherne GW. The ability to accumulate deoxyuridine triphosphate and cellular response to thymidylate synthase (TS) inhibition. Br J Cancer 2001;85(3):446–52.
[8] Webley SD, Hardcastle A, Ladner RD, Jackman AL, Aherne GW. Deoxyuridine triphosphatase (dUTPase) expression and sensitivity to the thymidylate synthase (TS) inhibitor ZD9331. Br J Cancer 2000;83(6):792–9.
[9] Houghton JA, Tillman DM, Harwood FG. Ratio of 2′-deoxyadenosine-5′-triphosphate/thymidine-5′-triphosphate influences the commitment

of human colon carcinoma cells to thymineless death. Clin Cancer Res 1995;1(7):723–30.
[10] Krokan HE, Drablos F, Slupphaug G. Uracil in DNA—occurrence, consequences and repair. Oncogene 2002;21(58):8935–48.
[11] Otterlei M, Warbrick E, Nagelhus TA, Haug T, Slupphaug G, Akbari M, et al. Post-replicative base excision repair in replication foci. EMBO J 1999;18(13):3834–44.
[12] Welsh SJ, Hobbs S, Aherne GW. Expression of uracil DNA glycosylase (UDG) does not affect cellular sensitivity to thymidylate synthase (TS) inhibition. Eur J Cancer 2003;39(3):378–87.
[13] Andersen S, Heine T, Sneve R, König I, Krokan HE, Epe B, et al. Incorporation of dUMP into DNA is a major source of spontaneous DNA damage, while excision of uracil is not required for cytotoxicity of fluoropyrimidines in mouse embryonic fibroblasts. Carcinogenesis 2005;26(3):547–55.
[14] Meyers M, Wagner MW, Mazurek A, Schmutte C, Fishel R, Boothman DA. DNA mismatch repair-dependent response to fluoropyrimidine-generated damage. J Biol Chem 2005;280(7):5516–26.
[15] Petronzelli F, Riccio A, Markham GD, Seeholzer SH, Stoerker J, Genuardi M, et al. Biphasic kinetics of the human DNA repair protein MED1 (MBD4), a mismatch-specific DNA *N*-glycosylase. J Biol Chem 2000;275(42):32422–9.
[16] Hardeland U, Bentele M, Jiricny J, Schar P. Separating substrate recognition from base hydrolysis in human thymine DNA glycosylase by mutational analysis. J Biol Chem 2000;275(43): 33449–56.
[17] Sobol RW, Kartalou M, Almeida KH, Joyce DF, Engelward BP, Horton JK, et al. Base excision repair intermediates induce p53-independent cytotoxic and genotoxic responses. J Biol Chem 2003;278(41):39951–9.
[18] Horton JK, Joyce-Gray DF, Pachkowski BF, Swenberg JA, Wilson SH. Hypersensitivity of DNA polymerase beta null mouse fibroblasts reflects accumulation of cytotoxic repair intermediates from site-specific alkyl DNA lesions. DNA Repair 2003;2(1):27–48.
[19] Li L, Berger SH, Wyatt MD. Involvement of base excision repair in response to therapy targeted at thymidylate synthase. Mol Cancer Ther 2004;3(6):747–53.
[20] Sobol RW, Horton JK, Kuhn R, Gu H, Singhal RK, Prasad R, et al. Requirement of mammalian DNA polymerase-beta in base-excision repair. Nature 1996;379(6561):183–6.
[21] Sobol RW, Prasad R, Evenski A, Baker A, Yang XP, Horton JK, et al. The lyase activity of the DNA repair protein beta-polymerase protects from DNA-damage-induced cytotoxicity. Nature 2000;405(6788): 807–10.
[22] Lavrik OI, Prasad R, Sobol RW, Horton JK, Ackerman EJ, Wilson SH. Photoaffinity labeling of mouse fibroblast enzymes by a base excision repair intermediate: Evidence for the role of poly(ADP-ribose) pol ymerase-1 in DNA repair. J Biol Chem 2001;276(27): 25541–8.
[23] Spanswick V, Hartley J, Ward T, Hartley J. Measurement of drug-induced DNA interstrand crosslinking using the single-cell gel electrophoresis (Comet) assay. In: Brown R, Boger-Brown U, editors. Cytotoxic Drug Resistance Mechanisms, vol. 28. Totowa, NJ: Humana Press; 1999. p. 143–54.
[24] Helma C, Uhl M. A public domain image-analysis program for the single-cell gel-electrophoresis (comet) assay. Mutat Res 2000;466(1):9–15.
[25] Mashiyama ST, Courtemanche C, Elson-Schwab I, Crott J, Lee BL, Ong CN, et al. Uracil in DNA, determined by an improved assay, is increased when deoxynucleosides are added to folate-deficient cultured human lymphocytes. Anal Biochem 2004;330(1):58–69.
[26] Freshney RI. Culture of Animal Cells. New York: Wiley-Liss, 2000.
[27] Mizushina Y, Takahashi N, Ogawa A, Tsurugaya K, Koshino H, Takemura M, et al. The cyanogenic glucoside, prunasin (D-mandelonitrile-beta-D-glucoside), is a novel inhibitor of DNA polymerase beta. J Biochem (Tokyo) 1999;126(2):430–6.
[28] Tomicic MT, Thust R, Sobol RW, Kaina B. DNA polymerase beta mediates protection of mammalian cells against ganciclovir-induced cytotoxicity and DNA breakage. Cancer Res 2001;61(20):7399–403.
[29] Ame JC, Spenlehauer C, de Murcia G. The PARP superfamily. Bioessays 2004;26(8):882–93.
[30] Babich MA, Day III RS. Potentiation of cytotoxicity by 3-aminobenzamide in DNA repair-deficient human tumor cell lines following exposure to methylating agents or anti-neoplastic drugs. Carcinogenesis 1988;9(4):541–6.
[31] Cleaver JE. Stimulation of repair replication by 3-aminobenzamide in human fibroblasts with ligase I deficiency. Carcinogenesis 1996;17(1):1–3.
[32] Le Page F, Schreiber V, Dherin C, De Murcia G, Boiteux S. Poly(ADP-ribose) polymerase-1 (PARP-1) is required in murine cell lines for base excision repair of oxidative DNA damage in the absence of DNA polymerase beta. J Biol Chem 2003;278(20):18471–7.
[33] Burkart V, Wang ZQ, Radons J, Heller B, Herceg Z, Stingl L, et al. Mice lacking the poly(ADP-ribose) polymerase gene are resistant to pancreatic beta-cell destruction and diabetes development induced by streptozocin. Nat Med 1999;5(3):314–9.
[34] Ha HC, Snyder SH. Poly(ADP-ribose) polymerase is a mediator of necrotic cell death by ATP depletion. Proc Natl Acad Sci USA 1999;96(24):13978–82.
[35] Canman CE, Tang HY, Normolle DP, Lawrence TS, Maybaum J. Variations in patterns of DNA damage induced in human colorectal tumor cells by 5-fluorodeoxyuridine: implications for mechanisms of resistance and cytotoxicity. Proc Natl Acad Sci USA 1992;89(21):10474–8.
[36] Ingraham HA, Dickey L, Goulian M. DNA fragmentation and cytotoxicity from increased cellular deoxyuridylate. Biochemistry 1986;25(11):3225–30.
[37] Yoshioka A, Tanaka S, Hiraoka O, Koyama Y, Hirota Y, Ayusawa D, et al. Deoxyribonucleoside triphosphate imbalance. 5-Fluorodeoxyuridine-induced DNA double strand breaks in mouse FM3A cells and the mechanism of cell death. J Biol Chem 1987;262(17):8235–41.
[38] Matsui SI, Arredondo MA, Wrzosek C, Rustum YM. DNA damage and p53 induction do not cause ZD1694-induced cell cycle arrest in human colon carcinoma cells. Cancer Res 1996;56(20):4715–23.
[39] Sedwick WD, Kutler M, Brown OE. Antifolate-induced misincorporation of deoxyuridine monophosphate into DNA: inhibition of high molecular weight DNA synthesis in human lymphoblastoid cells. Proc Natl Acad Sci USA 1981;78(2):917–21.
[40] Mishina Y, Ayusawa D, Seno T, Koyama H. Thymidylate stress induces homologous recombination activity in mammalian cells. Mutat Res 1991;246(1):215–20.
[41] Ayusawa D, Koyama H, Shimizu K, Kaneda S, Takeishi K, Seno T. Induction, by thymidylate stress, of genetic recombination as evidenced by deletion of a transferred genetic marker in mouse FM3A cells. Mol Cell Biol 1986;6(10):3463–9.
[42] Ayusawa D, Shimizu K, Koyama H, Takeishi K, Seno T. Accumulation of DNA strand breaks during thymineless death in thymidylate synthase-negative mutants of mouse FM3A cells. J Biol Chem 1983;258(20):12448–54.
[43] Ochs K, Lips J, Profittlich S, Kaina B. Deficiency in DNA polymerase beta provokes replication-dependent apoptosis via DNA breakage, Bcl-2 decline and caspase-3/9 activation. Cancer Res 2002;62(5):1524–30.
[44] Osheroff WP, Jung HK, Beard WA, Wilson SH, Kunkel TA. The fidelity of DNA polymerase beta during distributive and processive DNA synthesis. J Biol Chem 1999;274(6):3642–50.
[45] Schober C, Gibbs JF, Yin MB, Slocum HK, Rustum YM. Cellular heterogeneity in DNA damage and growth inhibition induced by ICI D1694, thymidylate synthase inhibitor, using single cell assays. Biochem Pharmacol 1994;48(5):997–1002.
[46] Tonkinson JL, Marder P, Andis SL, Schultz RM, Gossett LS, Shih C, et al. Cell cycle effects of antifolate antimetabolites: implications for

cytotoxicity and cytostasis. Cancer Chemother Pharmacol 1997;39(6):521–31.

[47] el-Hajj HH, Wang L, Weiss B. Multiple mutant of *Escherichia coli* synthesizing virtually thymineless DNA during limited growth. J Bacteriol 1992;174(13):4450–6.

[48] Barclay BJ, Little JG. Genetic damage during thymidylate starvation in *Saccharomyces cerevisiae*. Mol Gen Genet 1978;160(1):33–40.

[49] Barclay BJ, Kunz BA, Little JG, Haynes RH. Genetic and biochemical consequences of thymidylate stress. Can J Biochem 1982;60(3):172–84.

[50] Kunz BA, Haynes RH. DNA repair and the genetic effects of thymidylate stress in yeast. Mutat Res 1982;93:353–75.

[51] Tye BK, Nyman PO, Lehman IR, Hochhauser S, Weiss B. Transient accumulation of Okazaki fragments as a result of uracil incorporation into nascent DNA. Proc Natl Acad Sci USA 1977;74(1):154–7.